Journal of Operation and Automation in Power Engineering

Vol. XX, No. XX, XXXX, Pages: XXXX (Proofed)

http://joape.uma.ac.ir

Research Paper

Knowledge-Based Decentralized Arbitrage Coordination between Heavy-Duty Electric Truck Aggregators and Eco-Industrial Parks

Peyman Zare , *SeyedJalal SeyedShenava* * , and *Hossein Shayeghi*

Department of Electrical Engineering, Faculty of Engineering, University of Mohaghegh Ardabili, P.O. Box 179, Ardabil, Iran.

Abstract— *Existing studies on freight electrification largely rely on centralized architectures or simplified uncertainty models, leaving a gap in decentralized energy–mobility coordination under volatile electricity prices and privacy constraints. This study develops a decentralized optimization framework for coordinated operation of a heavy-duty electric truck aggregator and an eco-industrial park under concurrent market and fleet uncertainty. A hybrid distributionally robust–stochastic programming structure is adopted, where locational marginal price uncertainty is modeled through an uncertainty-budget robust layer, while fleet arrival, departure, and state-of-charge variability are represented via scenarios. The problem is decomposed using an alternating direction method of multipliers-based distributed algorithm to preserve autonomy and limit information exchange to tie-line power flows. Numerical results confirm stable convergence within approximately 130 iterations. When the price uncertainty budget spans the full 24-hour horizon, aggregator net profit decreases by 41% and eco-industrial park operating cost increases by 9% relative to deterministic pricing, without feasibility loss. The results demonstrate that integrating robust price hedging with stochastic fleet modeling enables economically consistent decentralized coordination under adverse market conditions.*

Keywords—Heavy duty electric trucks, coordinated aggregators, eco-industrial parks, e-mobility, stochastic.

NOMENCLATURE

Abbreviations

ADMM Alternating Direction Method of Multipliers
AGG Aggregator
CHP Combined Heat and Power
DRO Distributionally Robust Optimization
EIP Eco-Industrial Park
HDET Heavy-Duty Electric Truck
LMP Locational Marginal Price
RO Robust Optimization
SOC State of Charge
SP Stochastic Programming

Indices

$\mathcal{M}$ Set of HDET classes
$\mathcal{S}$ Set of stochastic scenarios
$\mathcal{T}$ Set of scheduling time intervals
a Index of wholesale electricity price uncertainty realization
b Index denoting the eco-industrial park entity
k Iteration counter in the ADMM algorithm
l Index of electrical load segments within the EIP
m Index of HDET class or group
s Scenario index in stochastic programming
t Discrete scheduling time interval (h)
t_s Time index for EIP operation (h)
t_{sm} Joint time–scenario index

Parameters

α ADMM penalty parameter
$\Delta_a^{\max}$ Maximum allowable LMP deviation (EUR/MWh)
η^{ch} Charging efficiency
η^{dch} Discharging efficiency
η_b Boiler thermal efficiency
η_e^{CHP} Electrical efficiency of the CHP unit
η_h^{CHP} Thermal efficiency of the CHP unit
Γ Uncertainty budget for robust price modeling
$\pi_t^{wm,0}$ Nominal wholesale electricity price (EUR/MWh)
ρ_s Probability of scenario s
AT_m Arrival time of HDET class m (h)
DT_m Departure time of HDET class m (h)
$E_{EIP}^{\max}$ Maximum energy level of the EIP storage system (kWh)
$E_{EIP}^{\min}$ Minimum energy level of the EIP storage system (kWh)
$E_m^{HDET,\max}$ Maximum battery energy of HDET class m (kWh)
$E_m^{HDET,\min}$ Minimum allowable battery energy of HDET class m (kWh)
$L_z^{\max}$ Capacity limit of the interconnecting tie-line (MW)
N_m^{HDET} Number of vehicles in HDET class m
$P_{EIP}^{ch,\max}$ Maximum charging power of EIP storage (MW)
$P_{EIP}^{dch,\max}$ Maximum discharging power of EIP storage (MW)
$P_m^{HDET,ch,\max}$ Maximum charging power of HDET class m (kW)

Variables

γ_{at} Price deviation decision variable (EUR/MWh)
λ_{tsm} ADMM dual variable for exchanged electricity
$\phi_{ts}^{EIP,ch}$ Binary indicator for EIP storage charging
$\phi_{ts}^{EIP,dch}$ Binary indicator for EIP storage discharging
ξ_{at} Dual variable in the robust price formulation
$E_{tsm}^{HDET,m}$ Battery energy level of HDET class m (kWh)
g_{ts}^b Natural gas input to the boiler (MW)

Received: 30 Dec. 2025
Revised: 14 Feb. 2026
Accepted: 09 May 2026
*Corresponding author:
E-mail: seyedshenava@uma.ac.ir (S.J. SeyedShenava)
DOI: 10.22098/joape.2026.19170.2494

g_{ts}^{CHP} Natural gas input to the CHP unit (MW)
h_{ts}^{b} Thermal output of the boiler (MW)
h_{ts}^{CHP} Thermal output of the CHP unit (MW)
$p_{tsm}^{AGG,wm}$ Power exchanged between the HDET aggregator and the wholesale market (MW)
$p_{tsm}^{AGG\rightarrow EIP}$ Electricity sold by the HDET aggregator to the EIP (MW)
$p_{tsm}^{EIP\rightarrow AGG}$ Electricity sold by the EIP to the HDET aggregator (MW)
$p_{tsm}^{HDET,m,ch}$ Charging power supplied to HDET class m (kW)
$p_{tsm}^{HDET,m,dch}$ Discharging power from HDET class m (kW)
p_{ts}^{CHP} Electrical output of the CHP unit (MW)
$p_{ts}^{EIP,ch}$ Charging power of EIP storage (MW)
$p_{ts}^{EIP,dch}$ Discharging power of EIP storage (MW)
$p_{ts}^{EIP,wm}$ Power exchanged between the EIP and the wholesale market (MW)
$u_{tsm}^{HDET,m,ch}$ Binary indicator for HDET charging state
$u_{tsm}^{HDET,m,dch}$ Binary indicator for HDET discharging state

1. Introduction

The electrification of freight transport is increasingly recognized as a critical pathway toward reducing emissions in energy-intensive industrial supply chains. Heavy-duty electric trucks are now being deployed at scale, particularly around logistics hubs and EIPs, where high energy demand, predictable traffic patterns, and access to grid infrastructure converge. At the same time, EIPs are evolving into complex multi-energy systems that integrate electricity, heat, gas, storage, and on-site generation, while actively participating in competitive wholesale electricity markets . These parallel developments create strong incentives for closer coordination between freight mobility and industrial energy systems, especially where electricity arbitrage and flexible demand can provide economic value [1].

A considerable amount of literature has examined freight electrification and its interaction with power system operation. Nevertheless, most studies remain centered on centralized coordination or simplified uncertainty treatments, offering limited insight into decentralized, market-facing energy–mobility coordination under volatile prices. As a result, arbitrage-oriented frameworks that preserve autonomy and data confidentiality remain underdeveloped. Infrastructure-oriented studies form an early foundation in this field. Ref. [2] analyzed the transition of heavy-duty fleets to electric operation through joint optimization of vehicles and charging infrastructure, although its conclusions depend strongly on assumed policy and deployment trajectories. Alonso-Villa *et al.* [3] addressed corridor-level fast-charging deployment under grid constraints, revealing sensitivity to localized demand and network conditions. Speth *et al.* [4] incorporated traffic flows and queuing limits into charger siting, yet excluded endogenous electricity price responses. Dimatulac *et al.* [5] quantified long-haul charging demand profiles and infrastructure needs, while abstracting from market participation and coordination mechanisms. Johansson *et al.* [6] formulated energy-aware routing for a single heavy-duty electric vehicle, but its limited scope restricts applicability to aggregator-based operation.

Operational control and flexibility valuation represent a second stream. Mahyari and Freeman [7] employed a sequential decision framework to balance fleet charging cost and service quality, relying on calibrated dynamics that may not generalize. Anderson *et al.* [8] embedded flexible charging and vehicle-to-grid operation into power system planning, but simplified fleet heterogeneity. Golab *et al.* [9] quantified the system value of commercial fleet flexibility under renewable variability, while leaving contractual and privacy constraints largely implicit. Syla *et al.* [10] compared smart charging and bidirectional operation under grid limits, without modeling decentralized negotiation among independent stakeholders.

A third group of studies focuses on electricity market participation and risk management. Wang *et al.* [11] examined risk-aware aggregator operation in ancillary service markets, yet remained detached from bilateral coordination with industrial systems. Pradana *et al.* [12] explored arbitrage-driven aggregator scheduling under price spreads, assuming sufficiently accurate market forecasts. Robbiano *et al.* [13] developed an uncertainty-aware energy management framework for aggregators, but abstracted from detailed industrial coupling. Audet *et al.* [14] introduced a distributionally robust bidding strategy to hedge price risk, operating primarily as a financial construct. Siqin *et al.* [15] extended robust bidding through a two-stage formulation under moment uncertainty, without accommodating mobility-specific constraints. Li *et al.* [16] proposed coordinated distributionally robust bidding across multiple markets, assuming a stable internal membership structure. Shen *et al.* [17] incorporated energy sharing and carbon transfer into uncertain bidding for integrated energy systems, while overlooking data confidentiality across independent entities. Lei *et al.* [18] presented a data-driven robust bidding strategy for shared storage, treating mobility demand as exogenous. Fatemi *et al.* [19] addressed privacy-preserving coordination via a bi-level structure, but focused on stationary storage assets rather than freight mobility.

Decentralized and privacy-preserving optimization has also received attention. Nafkha Tayari *et al.* [20] combined ADMM coordination with cryptographic protection, enabling confidentiality at the expense of computational overhead. Quteishat *et al.* [21] developed distributed stochastic energy management for coordinated microgrids, but employed uncertainty structures unsuited to logistics-driven fleets. Wang *et al.* [22] incorporated emission considerations into decentralized scheduling, while focusing on building-centric systems. Ref. [23] proposed a two-layer ADMM-based scheduling framework for low-carbon operation, simplifying market price dynamics. Fazlhashemi *et al.* [24] addressed decentralized risk-averse microgrid operation, without incorporating mobility aggregators as strategic agents. Zhang *et al.* [25] coordinated networked microgrids across multiple time scales, assuming stable participation sets. Kumar *et al.* [26] formulated decentralized control for infrastructure-coupled microgrids, yet omitted explicit arbitrage objectives. Ahmadi *et al.* [27] introduced user-centric decentralized energy management for communities, without bilateral industrial–mobility interaction. San Martín *et al.* [28] designed decentralized peer-to-peer trading with congestion awareness, while neglecting wholesale price arbitrage.

EIP energy systems form a final stream. Golshanfard *et al.* [29] addressed robust energy planning and operation in eco-industrial settings, treating transport electrification as an external load. Ref. [30] developed a robust low-carbon transition model for coupled eco-energy systems, without distributed implementation across privacy-constrained stakeholders. Fan *et al.* [31] co-optimized logistics scheduling and charging within industrial parks, but excluded explicit price hedging and robust market exposure. As a result, freight mobility remains weakly represented as an autonomous, market-facing actor in EIPs.

To summarize the literature review, Table 1 provides a taxonomy-based comparison of research studies and the present work across eight innovation-oriented dimensions derived from this paper.

Despite these contributions, important structural gaps remain. Existing ADMM-based decentralized energy management studies primarily focus on coordinated operation of microgrid clusters or community-level energy hubs under cooperative settings. In most cases, price signals are treated as deterministic or externally given, and the decision-makers do not act as autonomous market-facing agents engaged in bilateral electricity arbitrage As a result, the strategic interaction between independently owned industrial systems and mobility aggregators under volatile wholesale prices remains insufficiently addressed. Similarly, the distributionally robust and robust bidding literature largely emphasizes financial risk hedging in wholesale or ancillary service markets. These formulations typically abstract from detailed physical modeling of mobility systems and do not incorporate stochastic fleet dynamics such as arrival, departure, and state-of-charge variability. Consequently, robust price protection and high-fidelity mobility uncertainty are rarely integrated within a unified operational framework. This gap motivates the development of the proposed framework.

To address the identified gap, this study is guided by the following research questions:

1) Can decentralized bilateral electricity coordination between an HDET aggregator and an eco-industrial park remain economically viable under simultaneous wholesale price volatility and stochastic fleet behavior?
2) Does a hybrid robust–stochastic uncertainty structure provide structurally consistent protection against adverse price realizations while preserving high-fidelity mobility modeling?
3) Can an ADMM-based decomposition scheme ensure convergence and privacy preservation when autonomous market participants engage in strategic arbitrage?

This study develops a decentralized optimization framework for coordinating an HDET-AGG and an EIP under concurrent market and operational uncertainty. In contrast to prior works that rely on centralized control architectures, simplified uncertainty representations, or extensive information exchange, the proposed approach enables autonomous market participation, preserves data privacy, and explicitly addresses price risk within a bilateral electricity trading structure.

At the system level, two independently owned entities interact through bilateral electricity exchange while simultaneously participating in wholesale markets. A hybrid distributionally robust and stochastic programming structure is adopted to structurally distinguish wholesale price uncertainty from fleet-related operational uncertainty. Electricity price volatility is treated through an uncertainty-budget-based robust optimization layer, whereas uncertainty in truck arrival times, departure times, and initial states of charge is captured using scenario-based stochastic modeling. The resulting formulation is decomposed via an ADMM-based coordination scheme, enabling decentralized bilateral arbitrage with minimal information exchange restricted to interconnection power flows.

The main contributions of this research are outlined as follows:

1) A decentralized bilateral coordination framework is proposed for the joint operation of an HDET-AGG and an EIP, in which both entities act as autonomous market-facing participants while engaging in strategic electricity exchange.
2) An uncertainty-budget formulation is introduced to regulate exposure to LMP deviations, allowing both the HDET-AGG and the EIP to buy from and sell to the wholesale electricity market under adverse price realizations. The framework integrates a hybrid robust–stochastic programming structure that simultaneously captures worst-case wholesale price deviations and stochastic fleet behavior, thereby extending existing ADMM-based energy management and robust bidding models to a coupled industrial–mobility coordination context.

The remainder of the paper is organized as follows. Section 2 describes the coordinated interaction between the HDET aggregator and the EIP. Section 3 presents the optimization framework. Section 4 explains the computational solution approach. Section 5 discusses the numerical results, followed by concluding remarks in Section 6.

2. Coordinated Network of HDET aggregator and EIP

Fig. 1 shows a decentralized coordination between the HDET-AGG and an EIP within a single wholesale electricity market characterized by two zonal prices, LMP A and LMP-EIP. The HDET-AGG participates in the market at its zonal LMP, supplies electricity to HDET operators under a predefined tariff, and exchanges electricity with the EIP through a bilateral contract.

The EIP operates as a cost-minimizing energy consumer, procuring electricity from the wholesale market, purchasing natural gas, and trading electricity with the HDET-AGG. Thermal demand is supplied by a natural-gas-fired combined heat and power unit and an auxiliary boiler, while electrical demand is met through wholesale purchases, on-site CHP generation, discharge of the EIP storage system (EIPSS), and electricity obtained from the HDET-AGG.

Electricity exchanged between the entities is treated symmetrically as demand and generation, resulting in time-varying net electrical loads. Wholesale electricity may be directly consumed or stored in the EIPSS. Information exchange is restricted to traded electricity quantities to preserve privacy, and each entity independently optimizes its objective.

Energy exchanges are limited to electricity, as the HDET infrastructure does not interface with other carriers. Coordination is achieved using the alternating direction method of multipliers.

The HDET-AGG faces uncertainty in vehicle arrival, departure, and initial state of charge, while both entities are exposed to uncertain wholesale electricity prices. To avoid the computational burden of purely stochastic formulations, a hybrid distributionally robust–stochastic programming framework is adopted, modeling LMP uncertainty via robust optimization and HDET-related uncertainty through scenarios. Demand uncertainty is neglected due to its negligible variability relative to LMP fluctuations.

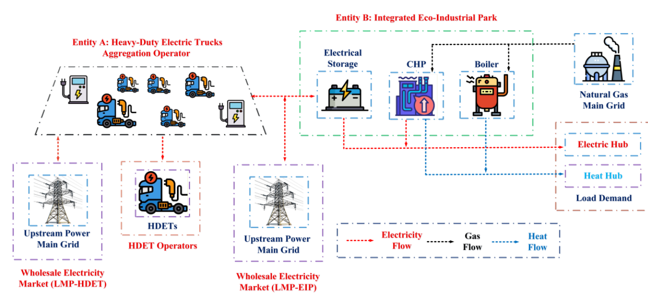

Fig. 1. Decentralized HDET aggregator–EIP coordination framework.

3. Knowledge-based Optimization Framework

Wholesale electricity price uncertainty and fleet-related operational uncertainty are treated separately in this framework because they arise from fundamentally different structural mechanisms. Locational marginal prices are determined outside the control of both the HDET-AGG and the EIP. They reflect market clearing outcomes and network conditions, and from the viewpoint of each entity they act as exogenous signals that may shift unfavorably regardless of internal scheduling decisions. Under such conditions, robust optimization offers a defensible hedging mechanism: it protects operational decisions against worst-case price deviations within a bounded uncertainty set, without imposing a specific probability distribution on short-term market fluctuations.

Fleet uncertainty has a different character. Arrival times, departure times, and initial states of charge are shaped by logistics and usage patterns that can be described through historical data and representative scenarios. These variations are operational rather than strategic; they do not emerge as adversarial market actions. A scenario-based stochastic formulation therefore retains the behavioral structure of mobility dynamics and aligns naturally with charging constraints and departure requirements.

Table 1. Taxonomy of selected research studies based on key innovation dimensions in decentralized energy–mobility coordination.

Ref.	Decentralized coordination	Bilateral electricity exchange	Hybrid RO–SP uncertainty	LMP uncertainty budgeting	Stochastic fleet modeling	ADMM-based decomposition	Privacy preserving exchange	Arbitrage oriented scheduling
[2]	×	×	×	×	×	×	×	×
[3]	×	✓	×	×	×	×	×	×
[4]	✓	✓	✓	✓	×	×	×	✓
[7]	✓	×	✓	✓	✓	×	✓	✓
[9]	✓	✓	✓	✓	×	✓	✓	✓
[11]	×	✓	×	✓	×	✓	✓	✓
[31]	×	✓	×	×	×	×	×	×
Present work	✓	✓	✓	✓	✓	✓	✓	✓

3.1. Decision model of the HDET aggregator

The HDET-AGG formulates its scheduling problem to minimize net operating expenditures, equivalently maximizing economic return, through coordinated participation in the wholesale electricity market, bilateral trading with the EIP, and retail electricity supply to HDETs. This objective is defined in Eq. (1). In each operating hour, the HDET-AGG may either sell electricity to or purchase electricity from the EIP at a pre-agreed contract price, while additional revenue is obtained from charging HDETs under a fixed tariff.

$$\min_{\phi_{tmon-a}} \sum_{s=1}^{S} \rho_s \sum_{m=1}^{M} N_{HDET,\mu,m}^{HDET} \{ \sum_{t=1}^{T} \pi_t^{con} (p_{tsm}^{EIP-HDET-AGG} - p_{tsm}^{HDET-AGG-EIP}) - \pi^s p_{tsm}^{s-HDET} + \max_{\phi_{tmon-a}} \sum_{t=1}^{T} \pi_t^{w-a} (p_{tsm}^{AG,b-g} - p_{tsm}^{AG,s-g}) \} \tag{1}$$

Wholesale electricity price volatility is handled via a robust optimization structure that enforces worst-case LMP realization through the third term of Eq. (1). The HDET battery state of charge evolves according to Eq. (2), with feasible limits imposed by Eq. (3) and departure requirements enforced by Eq. (4).

Group exits the charging facility with a fully charged battery at its designated departure time.

$$E_{tsm}^{HDET} = E_{t-1,sm}^{HDET} + \eta_{ch}^{HDET} p_{tsm}^{ch,HDET} - \frac{p_{tsm}^{dch,HDET}}{\eta_{dch}^{HDET}} \tag{2}$$

$$E_{\min^{HDET,m}} \leq E_{tsm}^{HDET,m} \leq E_{\max^{HDET,m}} \tag{3}$$

$$p_{tsm}^{s-HDET} = E_{\max^{HDET,m}} \qquad \forall t = DT \tag{4}$$

Charging energy supplied to the depot is sourced from electricity purchased from the wholesale market and from the EIP, as formalized in Eq. (5). Stored energy can be discharged and allocated to HDET users, exported to the wholesale market, or transferred to the EIP, as described in Eq. (6). The initial energy level of the charging facility is determined by the initial state of charge of each arriving HDET group.

$$p_{tsm}^{ch,HDET} = p_{tsm}^{AG,b-g} + p_{tsm}^{EIP-HDET-AGG} \tag{5}$$

$$p_{tsm}^{dch,HDET} = p_{tsm}^{s-HDET} + p_{tsm}^{AG,s-g} + p_{tsm}^{HDET-AGG-EIP} \tag{6}$$

Operational limits on charging and discharging rates are defined in Eqs. (7) and (8), respectively. A single HDET cannot be charged and discharged within the same time interval [32]. Electricity exchange between the HDET-AGG and the EIP takes place through a dedicated tie-line. The capacity limits of this interconnection are enforced in Eqs. (9) and (10), while Eqs. (11)-(13) ensures that buying and selling actions do not occur simultaneously.

$$E_{tsm}^{HDET} = E_{ini,sm}^{HDET} \qquad \forall t = AT \tag{7}$$

$$p_{\min^{ch,m}} u_{tsm}^{ch,HDET} \leq p_{tsm}^{ch,HDET} \leq p_{\max^{ch,m}} u_{tsm}^{ch,HDET} \quad \forall t \in [AT - DT] \tag{8}$$

$$p_{\min^{dch,m}} u_{tsm}^{dch,HDET} \leq p_{tsm}^{dch,HDET} \leq p_{\max^{dch,m}} u_{tsm}^{dch,HDET} \quad \forall t \in [AT - DT] \tag{9}$$

$$u_{tsm}^{ch,HDET} + u_{tsm}^{dch,HDET} \leq 1 \qquad \forall t \in [AT - DT] \tag{10}$$

$$p_{tsm}^{HDET-AGG-EIP} \leq L z_{tsm}^{HDET-AGG-EIP} \tag{11}$$

$$p_{tsm}^{EIP-HDET-AGG} \leq L^{\max} z_{tsm}^{EIP-HDET-AGG} \tag{12}$$

$$z_{tsm}^{HDET-AGG-EIP} + z_{tsm}^{EIP-HDET-AGG} \leq 1 \tag{13}$$

3.2. Operational representation of the EIP

The EIP is modeled as a cost-minimizing high-demand energy consumer that procures electricity at the applicable LMP, purchases natural gas, and engages in bilateral electricity trading with the HDET-AGG. Its objective, defined in Eq. (14), incorporates wholesale price uncertainty through a robust optimization mechanism that captures adverse LMP realizations.

$$\min \sum_{s=1}^{S} \rho_s \{ \sum_{t=1}^{T} \pi_t^{gas} g_{ts} + \max_{\phi_{wsm-b}} \sum_{t=1}^{T} \pi_t^{wm-b} (p_{ts}^{EIP,b-g} - p_{ts}^{EIP,s-g}) \} \tag{14}$$

The internal electrical and thermal energy balances of the EIP are defined in Eqs. (15) and (16). Natural gas inflow supplies both the combined heat and power unit and the auxiliary boiler, as stated in Eq. (17). Heat generation through the boiler is modeled in Eq. (18), while the coupled production of electricity and heat via the CHP unit is described in Eqs. (19) and (20) [33].

$$
\begin{aligned}
&p_{ts}^{wm,l} + p_{ts}^{CHP} + p_t^{dch,EIP} + \\
&\sum_{m=1}^{M} N_{HDET,\mu,m} p_{tsm}^{HDET-AGG-EIP} = ED_t + \\
&\sum_{m=1}^{M} N_{HDET,\mu,m} p_{tsm}^{EIP-HDET-AGG} + p_{ts}^{EIP,s-g}
\end{aligned} \tag{15}
$$

$$
h_{ts}^{b} + h_{ts}^{CHP} = HD_t \tag{16}
$$

$$
g_{ts} = g_{ts}^{CHP} + g_{ts}^{b} \tag{17}
$$

$$
h_{ts}^{b} = \eta^{b} g_{ts}^{b} \tag{18}
$$

$$
p_{ts}^{CHP} = \eta_e^{CHP} g_{ts}^{CHP} \tag{19}
$$

$$
h_{ts}^{CHP} = \eta_h^{CHP} g_{ts}^{CHP} \tag{20}
$$

Energy storage dynamics within the EIP are captured through the EIP storage system balance in Eq. (21). Limits on the state of charge, charging power, and discharging power are imposed through Eqs. (22), (23), and (24). Mutual exclusivity between charging and discharging modes is enforced by Eq. (25). Electricity purchased from the wholesale market may either be stored in the EIPSS or delivered directly to the load, as specified in Eq. (26).

$$
\begin{aligned}
&E_{ts}^{EIP} = E_{t-1,s}^{EIP} + \eta_{ch}^{EIP} p_{ts}^{ST} - \\
&p_{ts}^{dch,EIP} / \eta_{dch}^{EIP}
\end{aligned} \tag{21}
$$

$$
E_{\min^{EIP}} \leq E_{ts}^{EIP} \leq E_{\max^{EIP}} \tag{22}
$$

$$
p_{ts}^{ST} \leq p_{\max^{ch,EIP}} a_{ts}^{ch,EIP} \tag{23}
$$

$$
p_{ts}^{dch,EIP} \leq p_{\max^{dch,EIP}} a_{ts}^{dch,EIP} \tag{24}
$$

$$
a_{ts}^{ch,EIP} + a_{ts}^{dch,EIP} \leq 1 \tag{25}
$$

$$
p_{ts}^{EIP,b-g} = p_{ts}^{ST} + p_{ts}^{wm,l} \tag{26}
$$

Electricity exchanged with the HDET-AGG is constrained by the tie-line capacity limits in Eqs. (27) and (28). Simultaneous electricity purchase and sale between the two entities is prevented by Eq. (29).

$$
\begin{aligned}
&p_{tsm}^{HDET-AGG-EIP} \leq \\
&L_{tsm}^{\max,HDET-AGG-EIP} v_{tsm}^{HDET-AGG-EIP}
\end{aligned} \tag{27}
$$

$$
\begin{aligned}
&p_{tsm}^{EIP-HDET-AGG} \leq \\
&L_{tsm}^{\max,EIP-HDET-AGG} v_{tsm}^{EIP-HDET-AGG}
\end{aligned} \tag{28}
$$

$$
v_{tsm}^{HDET-AGG-EIP} + v_{tsm}^{EIP-HDET-AGG} \leq 1 \tag{29}
$$

The CHP unit is further characterized by its feasible operation region, which captures the inherent coupling between electrical and thermal outputs. This region defines a closed set of admissible operating points. The mathematical constraints defining this region are provided in Eqs. (30)-(34).

$$
p_{ts}^{CHP} - P^{A} - \frac{P^{A} - P^{B}}{Q^{A} - Q^{B}} \left(h_{ts}^{CHP} - Q^{A} \right) \leq 0 \tag{30}
$$

$$
\begin{aligned}
&p_{ts}^{CHP} - P^{B} - \\
&\tfrac{P^{B} - P^{C}}{Q^{B} - Q^{C}} \left(h_{ts}^{CHP} - Q^{B} \right) \geq -(1 - v_{ts}^{CHP}) M
\end{aligned} \tag{31}
$$

$$
\begin{aligned}
&p_{ts}^{CHP} - P^{C} - \\
&\tfrac{P^{C} - P^{D}}{Q^{C} - Q^{D}} \left(h_{ts}^{CHP} - Q^{C} \right) \geq -(1 - v_{ts}^{CHP}) M
\end{aligned} \tag{32}
$$

$$
0 \leq h_{ts}^{CHP} \leq H^{B} v_{ts}^{CHP} \tag{33}
$$

$$
0 \leq p_{ts}^{CHP} \leq P^{A} v_{ts}^{CHP} \tag{34}
$$

3.3. Robust modeling of wholesale electricity price uncertainty

Wholesale electricity price uncertainty for both entities is modeled through a robust optimization framework. The HDET-AGG and the EIP interact with the wholesale market under LMP A and LMP-EIP, respectively, with price deviations driven toward adverse realizations. Eq. (35) maximizes LMP deviations from expected values, which are incorporated into effective market prices through Eq. (36).

$$
\begin{aligned}
&\max_{\phi_t^{\pi^{wm0a}}} \sum_{t=1}^{T} \pi_t^{wm0a} \left(p_{tsm}^{AG,b-g} - p_{tsm}^{AG,s-g} \right), \\
&\forall t = 1, \ldots, T
\end{aligned} \tag{35}
$$

$$
\pi_t^{wm0a} = \bar{\pi}_t^{wm0a} + \phi_t^{a}, \qquad \phi_t^{a} \in \Re, \qquad \forall t = 1, \ldots, T. \tag{36}
$$

The deviation variable is permitted to take either positive or negative values, and the aggregate magnitude of uncertainty is restricted through the uncertainty budget constraints in Eqs. (37) and (38). The presence of absolute value terms in Eqs. (37) and (38) introduces nonlinearity into the formulation. The linearization technique described in the Appendix B is applied to address this issue.

$$
\begin{aligned}
&|\phi_t^{a}| \leq \Delta_{\max^{AG}} \bar{\pi}_t^{wm0a}, \qquad \varphi_t^{a} \leq 0, \\
&\varphi_t^{a} \geq 0, \qquad \forall t = 1, \ldots, T
\end{aligned} \tag{37}
$$

$$
\begin{aligned}
&\sum_{t=1}^{T} |\phi_t^{a}| \leq \Gamma^{a}, \qquad \sigma_t^{a} \geq 0,\ \sigma_t^{a} \in \Re, \qquad \forall t = 1, \ldots, T \\
&\Gamma^{a} = N_p \Delta_{\max^{AG}} \frac{\sum_{t=1}^{T} \bar{\pi}_t^{wm0a}}{T}.
\end{aligned} \tag{38}
$$

Subsequently, application of the duality theorem yields an equivalent minimization form of the objective function in Eq. (39). The associated dual constraints are presented in Eqs. (40)-(43).

$$
\min \sum_{t=1}^{T} \begin{pmatrix} \bar{\pi}_t^{wm0a} \xi_t^{a} + \Delta_{\max^{AG}} \bar{\pi}_t^{wm0a} \bar{\varphi}_t^{a} - \\ \Delta_{\max^{AG}} \bar{\pi}_t^{wm0a}{}_t^{a} + \Gamma^{a} \bar{\omega}^{a} \end{pmatrix} \tag{39}
$$

$$\xi_t^a \geq \sum_{s=1}^{S} \rho_s \sum_{m=1}^{M} N_{HDET,\mu,m} \left(p_{tsm}^{AG,b-g} - p_{tsm}^{AG,s-g} \right) \tag{40}$$

$$-\xi_t^a + \bar{\varphi}_t^a +_t^a + \sigma_t^a = 0 \tag{41}$$

$$-\sigma_t^a + \bar{\omega}^a \geq 0 \tag{42}$$

$$\sigma_t^a + \bar{\omega}^a \geq 0 \tag{43}$$

A corresponding minimization formulation and constraint set are derived for the EIP, identified as entity B, and are reported in Eqs. (44)-(48).

$$\min \sum_{t=1}^{T} \begin{pmatrix} \bar{\pi}_t^{wm0b} \xi_t^b + \Delta_{\max^{EH}} \bar{\pi}_t^{wm0b} \bar{\varphi}_t^b - \\ \Delta_{\max^{EH}} \bar{\pi}_t^{wm0b}{}_t^b + \Gamma^b \bar{\omega}^b \end{pmatrix} \tag{44}$$

$$\xi_t^b \geq \sum_{s=1}^{S} \rho_s \left(p_{ts}^{EIP,b-g} - p_{ts}^{EIP,s-g} \right) \tag{45}$$

$$-\xi_t^b + \bar{\varphi}_t^b +_t^b + \sigma_t^b = 0 \tag{46}$$

$$-\sigma_t^b + \bar{\omega}^b \geq 0 \tag{47}$$

$$\sigma_t^b + \bar{\omega}^b \geq 0. \tag{48}$$

4. Computational resolution approach

4.1. ADMM-driven coordination mechanism

The alternating direction method of multipliers is used to coordinate a small number of decentralized decision-makers under limited information sharing. Following the canonical ADMM formulation in [34], the coupled objectives are linked by an equality constraint in Eq. (49). The augmented Lagrangian is defined in Eq. (50), with independent primal updates in Eqs. (51) and (52), and a dual update in Eq. (53).

$$\min\ f(x) + g(z) \quad \forall x \in X,\ z \in Z \quad \text{s.t.} Ax + Bz = c \tag{49}$$

$$\begin{aligned} &\min\ L_\alpha(x, z, y) = \\ &f(x) + g(z) + y^\top (Ax + Bz - c) + \\ &\tfrac{\alpha}{2} \| Ax + Bz - c \|^2, \qquad \forall x \in X,\ z \in Z \end{aligned} \tag{50}$$

$$x^{k+1} = \arg\min_x L_\alpha \left(x, z^k, y^k \right) \tag{51}$$

$$z^{k+1} = \arg\min_z L_\alpha \left(x^{k+1}, z, y^k \right) \tag{52}$$

$$\begin{aligned} &y^{k+1} = \\ &y^k + \alpha \left(Ax^{k+1} + Bz^{k+1} - c \right), \qquad \forall x \in X,\ z \in Z \end{aligned} \tag{53}$$

4.2. Distributed operating structure of the EIP and HDET aggregator

Centralized coordination assumes a single authority, which is impractical when the EIP and HDET charging infrastructure are owned by separate stakeholders. In practice, privacy and communication constraints limit information exchange to boundary quantities only [35], necessitating decentralized solution approaches. ADMM addresses this requirement by decomposing separable large-scale optimization problems into cooperative local sub-problems.

In the proposed framework, the EIP and the HDET-AGG independently optimize their internal decisions, sharing only the electricity exchanged through the tie-line in Fig. 1. ADMM iteratively adjusts these exchanged quantities to reconcile bilateral trade inconsistencies while preserving operational autonomy. The resulting local sub-problems are defined below.

A) HDET aggregator sub-problem within the ADMM scheme

The HDET-AGG engages with the wholesale electricity market at LMP A, conducts bilateral electricity transactions with the EIP, and supplies power to HDET users. Its local optimization minimizes total operating cost while explicitly incorporating the exchanged electricity with the EIP. Within the ADMM framework, the HDET-AGG objective is reformulated accordingly. The term representing wholesale market transactions is replaced by the equivalent dual expression obtained in Eq. (39), yielding the modified objective in Eq. (54). The resulting problem is solved subject to constraints Eqs. (2)-(13) and Eqs. (40)-(43).

$$\begin{aligned} &\min \sum_{s=1}^{S} \rho_S \Bigg\{ \sum_{m=1}^{M} N_{HDET,\mu,m} \Bigg[\sum_{t=1}^{T} \pi_t^{con} \big(p_{tsm}^{EIP-HDET-AGG} - \\ &p_{tsm}^{HDET-AGG-EIP} \big) - \pi^{s-HDET} p_{tsm}^{s-HDET} + \\ &\sum_{t=1}^{T} \left(\bar{\pi}_t^{wm0a} \xi_t^a + \Delta_{\max^{AG}} \bar{\pi}_t^{wm0a} \bar{\varphi}_t^a - \Delta_{\max^{AG}} \bar{\pi}_t^{wm0a} \bar{\varphi}_t^a + \Gamma^a \bar{\omega}^a \right) + \\ &\sum_{m=1}^{M} \Big[\gamma_{tsm}^{1,k+1} \left(p_{tsm}^{HDET-AGG-EIP} - \bar{p}_{tsm}^{HDET-AGG-EIP} \right) + \\ &\gamma_{tsm}^{2,k+1} \left(p_{tsm}^{EIP-HDET-AGG} - \bar{p}_{tsm}^{EIP-HDET-AGG} \right) + \\ &\tfrac{\alpha}{2} \left\| p_{tsm}^{HDET-AGG-EIP} - \bar{p}_{tsm}^{HDET-AGG-EIP} \right\|^2 + \\ &\tfrac{\alpha}{2} \left\| p_{tsm}^{EIP-HDET-AGG} - \bar{p}_{tsm}^{EIP-HDET-AGG} \right\|^2 \Big] \Bigg\} \end{aligned} \tag{54}$$

B) EIP sub-problem within the ADMM scheme

For the EIP, the augmented Lagrangian component is appended to the original objective function defined in Eq. (14). As with the HDET-AGG, the wholesale market trading cost is substituted by its dual counterpart derived in Eq. (44). This leads to the revised EIP objective expressed in Eq. (55). The EIP sub-problem is solved under the constraints specified in Eqs. (15)-(34) and Eqs. (45)-(48).

$$\begin{aligned}
&\min \sum_{s=1}^{S} \rho_s \{ \sum_{t=1}^{T} \pi_t^{gas} g_{ts} + \\
&\sum_{t=1}^{T} (\bar{\pi}_t^{wm0b} \xi_t^b + \Delta_{\max^{EIP}} \bar{\pi}_t^{wm0b} \bar{\varphi}_t^b - \Delta_{\max^{EIP}} \bar{\pi}_t^{wm0b} \underline{\varphi}_t^b + \Gamma^b \bar{\omega}^b) \\
&+ \sum_{m=1}^{M} [\gamma_{tsm}^{1,k+1} \left(p_{tsm}^{HDET-AGG-EIP} - \bar{p}_{tsm}^{HDET-AGG-EIP} \right) + \\
&\gamma_{tsm}^{2,k+1} \left(p_{tsm}^{EIP-HDET-AGG} - \bar{p}_{tsm}^{EIP-HDET-AGG} \right) + \\
&\tfrac{\alpha}{2} \left\| p_{tsm}^{HDET-AGG-EIP} - \bar{p}_{tsm}^{HDET-AGG-EIP} \right\|^2 + \\
&\tfrac{\alpha}{2} \left\| p_{tsm}^{EIP-HDET-AGG} - \bar{p}_{tsm}^{EIP-HDET-AGG} \right\|^2] \}
\end{aligned} \tag{55}$$

C) Iterative decentralized coordination procedure

Given the two local optimization problems, the ADMM-based coordination proceeds through a fixed sequence of steps. First, the exchanged electricity variables associated with the EIP, the iteration index, and the dual variable are initialized to zero. Next, the HDET-AGG sub-problem in Eq. (54) is solved. The EIP sub-problem in Eq. (55) is then addressed. Following these updates, the dual variable, corresponding to the Lagrange multiplier of the exchanged electricity constraint, is updated using Eq. (56). Convergence is subsequently assessed using the criteria defined in Eqs. (57) and (58). Satisfaction of these conditions terminates the process; otherwise, the algorithm returns to the second step and continues iterating.

The overall sequence of the decentralized coordination is illustrated in Fig. 2, where the robust optimization layer and the ADMM-based iterative process are shown as distinct components.

$$\left| \begin{aligned}
&\gamma_{tsm}^{1,k+1} = \gamma_{tsm}^{1,k} + \alpha \left(p_{tsm}^{HDET-AGG-EIP} - \bar{p}_{tsm}^{HDET-AGG-EIP} \right) \\
&\gamma_{tsm}^{2,k+1} = \gamma_{tsm}^{2,k} + \alpha \left(p_{tsm}^{EIP-HDET-AGG} - \bar{p}_{tsm}^{EIP-HDET-AGG} \right)
\end{aligned} \right. \tag{56}$$

$$\begin{aligned}
&Diff^{HDET-AGG-EIP} = \\
&\sum_{s=1}^{S} \rho_s \sum_{m=1}^{M} N_{HDET,\mu,m} \sum_{t=1}^{T} \left| p_{tsm}^{HDET-AGG-EIP}(k) - p_{tsm}^{HDET-AGG-EIP}(k+1) \right|
\end{aligned} \tag{57}$$

$$\left| \begin{aligned}
&Diff^{EIP-HDET-AGG} = \\
&\sum_{s=1}^{S} \rho_s \sum_{m=1}^{M} N_{HDET,\mu,m} \sum_{t=1}^{T} \left| p_{tsm}^{EIP-HDET-AGG}(k) - \right. \\
&\left. p_{tsm}^{EIP-HDET-AGG}(k+1) \right| \\
&Diff^{(k)} = \\
&\max \left(\left| Diff^{HDET-AGG-EIP} \right|, \left| Diff^{EIP-HDET-AGG} \right| \right) \leq \varepsilon
\end{aligned} \right. \tag{58}$$

5. Results and Discussion

Numerical simulations are conducted using the structure depicted in Fig. 1 to assess the proposed framework. The decentralized scheduling of the HDET-AGG and the EIP is formulated through a hybrid DRO–SP approach over a 24 h operating horizon. Input data are drawn from well-established sources to ensure realistic

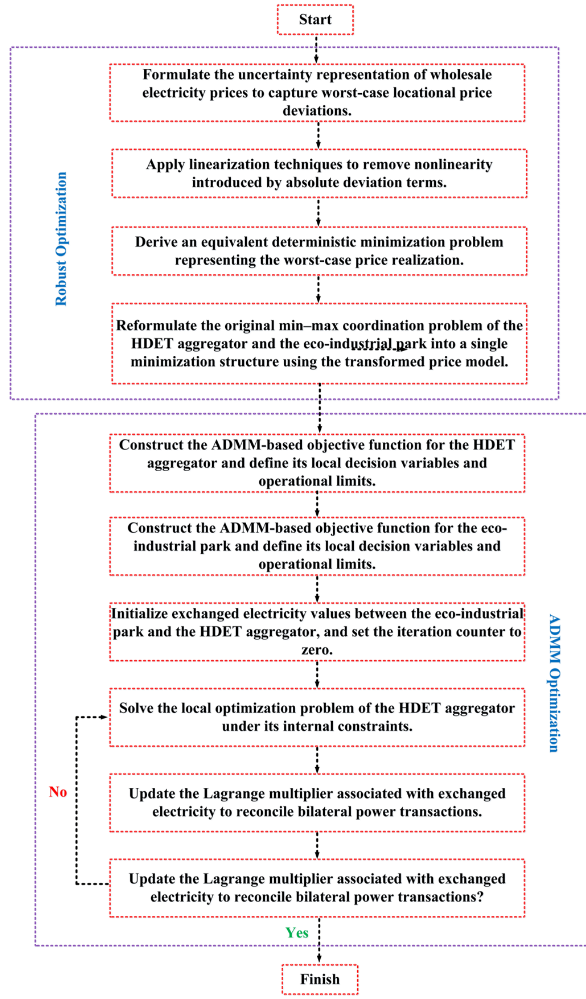

Fig. 2. Iterative decentralized coordination framework based on ADMM and robust optimization.

operating conditions. Fleet behavior, particularly connection and disconnection timing at the charging facility together with the initial battery state of HDETs, exerts a strong influence on scheduling outcomes. For this reason, uncertainty associated with HDET behavior is explicitly represented through a stochastic programming layer.

The reduced scenario set adopted from [36] is summarized in Table 2. Scenarios are generated using a Gaussian-based sampling method. The earliest connection is assumed at time step 5 of the daily horizon, while the latest disconnection occurs at time step 22. For simplicity, each HDET is considered to remain connected to the charging infrastructure throughout its stay. The main technical characteristics of the five representative HDET categories examined in this study are reported in Table 3 [36]. The total fleet size is fixed at 2000 HDET. Nevertheless, the number of connected HDETs varies over time and depends on scenario-specific arrival and departure patterns [37]. As these patterns differ across scenarios, the connected fleet size evolves dynamically during the day.

The electricity tariff offered to HDET operators is assumed constant at 30.10 EUR/MWh [37]. Wholesale market price signals illustrated in Fig. 3-(a) are taken from [38] and treated as expected values within the robust optimization framework. During the early and late portions of the daily horizon, corresponding to time steps 1–7 and 19–24, the locational marginal price at the HDET aggregator node (LMP-HDET) exceeds the locational marginal price at the EIP node (LMP-EIP). Accordingly, the bilateral electricity trading price between the two entities is set equal to the average of LMP-HDET and LMP-EIP.

Electricity and thermal demand profiles of the EIP are shown in Fig. 3-(b). Given that gas price fluctuations within a single-day horizon are negligible, the gas price is assumed constant at 18.92 EUR/MWh [39]. The boiler capacity is selected to match the peak thermal demand, while the feasible operation region parameters of the CHP unit are adopted from [40]. Additional characteristics of the case study are provided in Appendix A. The resulting mixed-integer quadratic conic programming formulation is solved using the CBC solver implemented in Python.

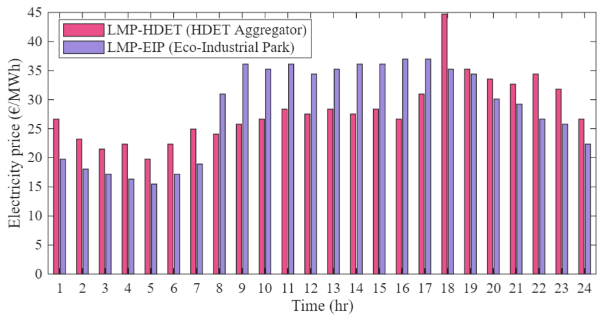

(a) Hourly wholesale electricity prices for HDET-AGG and EIP.

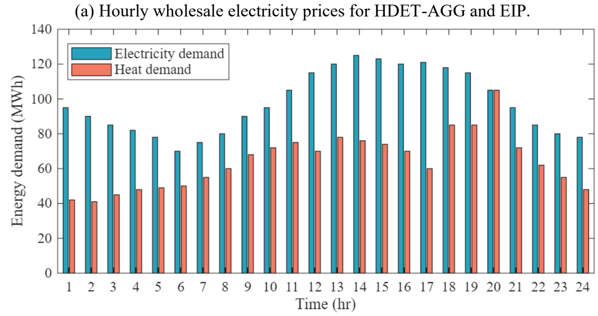

(b) Electricity and thermal demand of the eco-industrial park.

Fig. 3. Market prices and EIP demand profiles.

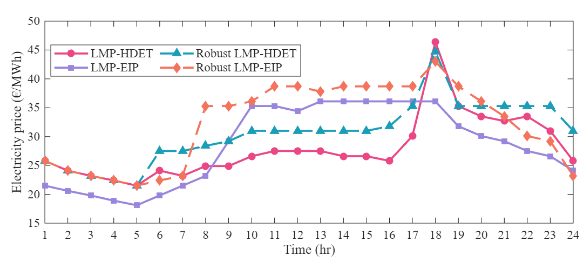

(a). Expected and robust LMPs at HDET-AGG and EIP nodes.

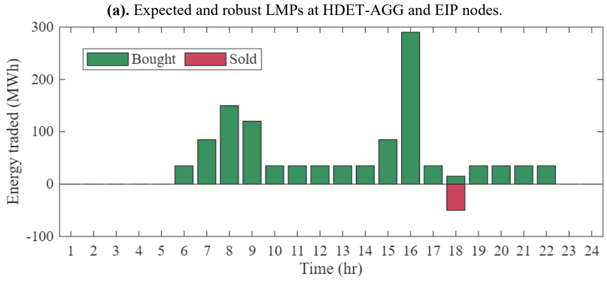

(b). Electricity trading of the HDET aggregator with the wholesale market.

Fig. 4. Robust price signals and market transactions.

This section presents an additional numerical examination of the hybrid DRO–SP framework, with emphasis on the interaction between robust pricing signals and decentralized operational decisions. Fig. 4-(a) contrasts the nominal and worst-case locational marginal prices. At the node associated with the HDET aggregator, denoted as LMP-HDET, the robust price profile remains flat during the initial and terminal portions of the daily horizon, specifically across slots 1–6 and 22–24. This outcome is a direct consequence of fleet availability constraints. No HDETs are connected to the charging infrastructure before slot 5, and no departures are scheduled beyond slot 22.

The temporal discretization of the model introduces a subtle but relevant effect. Although trucks connect to the system immediately upon arrival, their charging power is reflected only in the following hourly interval. As a result, vehicles arriving during slot 5 contribute to charging decisions from slot 6 onward. Outside the boundary intervals, LMP-HDET exhibits an upward shift under the robust setting, with the sole exception occurring at slot 18. As indicated in Fig. 4-(b), this slot corresponds to the only period in which the aggregator exports electricity to the wholesale market. In all remaining slots, the aggregator acts as a net importer. The robust formulation therefore amplifies prices during purchase periods and depresses them during sales, capturing the adverse realization of market uncertainty.

The robust price trajectory at the EIP node, labeled LMP-EIP, follows a different pattern. As shown in Fig. 4-(a), LMP-EIP generally increases toward unfavorable values because the EIP predominantly procures electricity from the wholesale market and rarely exports power, consistent with the exchange pattern reported in Fig. 5-(a). This behavior is further clarified by Fig. 5-(b), which shows that during slots 8–15 the EIP requires external electricity to satisfy its internal load. Conversely, electricity is exported to the HDET-AGG during slots 6, 7, 18, 20, and 22, when the aggregator's offered price exceeds the prevailing wholesale level.

The departure constraint imposed by Eq. (4) obliges the HDET-AGG to deliver fully charged batteries at the time of vehicle exit. This requirement is validated in Fig. 5-(c), where energy delivery to HDET owners is concentrated in the departure window spanning slots 17–22.

The aggregate charging and discharging behavior of the truck batteries is depicted in Fig. 6-(a). Most discharging aligns with vehicle departures, while additional discharge occurs during slots 8–16 when electricity is transferred to the EIP. Charging events coincide with periods in which power is imported either from the EIP or directly from the wholesale market.

Operation of the EIP storage system is illustrated in Fig. 6-(b). The storage unit absorbs electricity during low-price intervals of LMP-EIP and releases energy during high-price periods, indicating economically driven arbitrage.

Table 4 examines the response of the proposed framework to different sizes of the LMP uncertainty budget, expressed as the number of hourly periods exposed to price deviations over the daily horizon. When uncertainty is absent, the system operates under fully deterministic prices. As the share of uncertain hours expands to cover the entire day, clear economic shifts emerge. The aggregator's profit decreases by approximately 41% across the examined range, while the total operating cost of the EIP increases by about 9%.

This opposite movement reflects the conservative adjustment of effective electricity prices as more hours are protected against unfavorable realizations. With a larger uncertainty budget, the optimization anticipates higher purchase prices and lower selling prices during a greater portion of the day. As a result, the aggregator experiences a progressive erosion of margins, whereas the EIP faces higher procurement expenses due to increased reliance on costly wholesale electricity.

Despite these changes, the model remains feasible for all uncertainty levels considered. This indicates structural robustness under increasingly adverse price assumptions. The reason is straightforward. The formulation is designed to hedge against the worst admissible price outcomes. If the system can operate when prices are maximally unfavorable, it will necessarily remain viable

Table 2. Scenario-based characterization of HDET arrival, departure, and initial battery conditions.

Scenario ID	Scenario description	Initial battery state of HDETs	Arrival time (AT) (h)	Departure time (DT) (h)
S_1	Early-morning depot entry with low initial charge	0.25	5	21
S_2	Early arrival with moderate initial charge	0.38	6	20
S_3	Morning arrival with partially charged fleet	0.47	7	19
S_4	Standard working-day arrival pattern	0.52	8	18
S_5	Late-morning arrival with high initial charge	0.65	9	18
S_6	Midday arrival with moderate reserve	0.41	11	19
S_7	Afternoon arrival with low reserve state	0.22	13	22
S_8	Afternoon arrival with heterogeneous charge levels	0.34	14	22
S_9	Evening arrival with high reserve	0.71	16	23
S_{10}	Night arrival with constrained parking duration	0.29	18	24

Table 3. Operational and battery characteristics of representative HDET classes.

Attribute	HDET class 1	HDET class 2	HDET class 3	HDET class 4	HDET class 5
Nominal charging–discharging power limit (kW)	18.0	16.8	21.0	12.0	13.2
Maximum usable battery capacity (kWh)	108	96	44	42	27
Share of trucks in the aggregated fleet	0.22	0.18	0.16	0.26	0.18

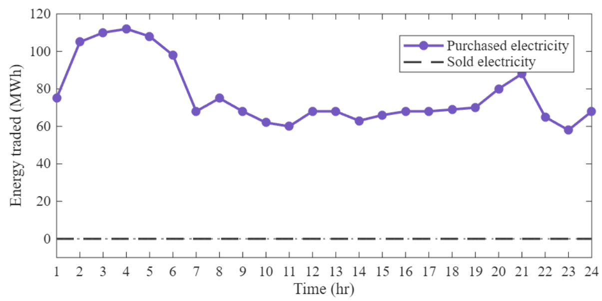

(a). EIP–wholesale market trading.

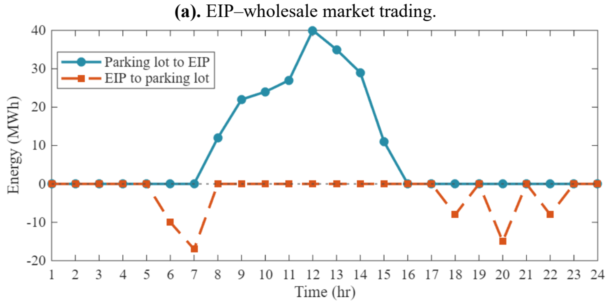

(b). Electricity exchange between entities.

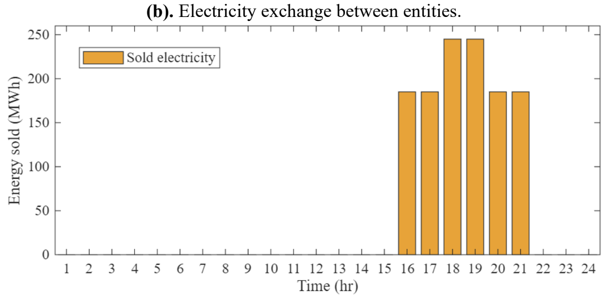

(c). Electricity supplied to HDETs.

Fig. 5. Electricity exchange profiles.

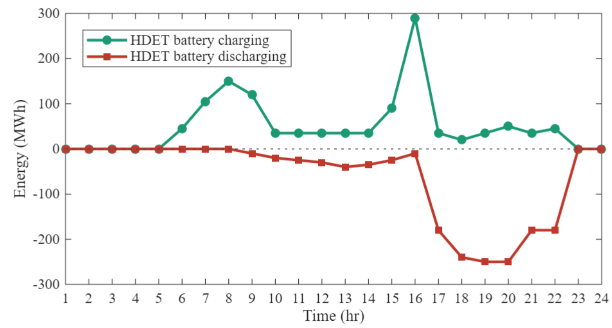

(a). Aggregated HDET battery operation.

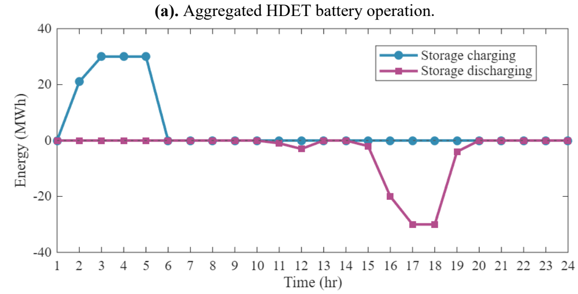

(b). EIP storage charging and discharging.

Fig. 6. Batteries charging and discharging profiles.

Table 4. Sensitivity of system economics to LMP uncertainty budget.

Metric \ Uncertainty budget level	0	6	12	18	24
Aggregator net profit (EUR)	13,125	10,441	7,886	7,785	7,729
EIP total operating cost (EUR)	97,753	101,701	103,983	106,640	106,912

under any less severe realization. From an economic perspective, this mirrors rational market behavior, where buyers plan for high prices and sellers prepare for low ones.

Overall, the sensitivity analysis demonstrates that enlarging the LMP uncertainty budget leads to predictable percentage shifts in costs and profits, without compromising solvability. The results confirm that the proposed approach can accommodate substantial price uncertainty while maintaining consistent operational decisions.

To enhance reproducibility and clarify parameter selection, additional sensitivity analysis is conducted on three key parameters: the LMP uncertainty budget (Γ), the ADMM penalty parameter (α), and the convergence tolerance (ε). The baseline configuration follows (Γ = 12 h, α = 1, ε = 0.001). Table 5 reports the resulting economic and convergence indicators.

Table 5 confirms that economic results are primarily sensitive to the uncertainty budget Γ, while ADMM parameters mainly affect convergence behavior. Reducing Γ from 12 to 6 hours increases aggregator profit from 7,886 EUR to 10,441 EUR and lowers EIP cost from 103,983 EUR to 101,701 EUR, reflecting reduced conservatism. Increasing Γ to 18 hours decreases profit to 7,785 EUR and raises EIP cost to 106,640 EUR, consistent with stronger worst-case price protection.

Variations in the ADMM penalty parameter α do not alter

Table 5. Sensitivity of economic outcomes and convergence to key parameters.

Case	**Γ (h)**	α	ε	**Aggregator net profit (EUR)**	**EIP operating cost (EUR)**	**Iterations to convergence**
Base	12	1.0	0.001	7,886	103,983	128
A_1	6	1.0	0.001	10,441	101,701	124
A_2	18	1.0	0.001	7,785	106,640	132
B_1	12	0.5	0.001	7,886	103,983	176
B_2	12	2.0	0.001	7,886	103,983	109
C_1	12	1.0	0.0005	7,886	103,983	141
C_2	12	1.0	0.0001	7,886	103,983	188

Table 6. Scalability assessment under expanded fleet size, extended horizon, and multiple aggregators.

Case	**Fleet size (HDETs)**	**Horizon (h)**	**Number of aggregators**	**Scenarios (S)**	**ADMM iterations**	**Total solve time (s)**
Base	2000	24	1	10	130	180
F_1	4000	24	1	10	134	355
F_2	6000	24	1	10	138	525
H_1	2000	48	1	10	142	365
H_2	2000	72	1	10	153	560
A_1	2000 (1000+1000)	24	2	10	156	265
A_2	2000 (700+650+650)	24	3	10	171	345
AH_1	4000 (2000+2000)	48	2	10	188	780

economic outcomes, as expected from the decomposition structure; however, convergence speed improves when α increases from 0.5 to 2.0. Similarly, tighter convergence tolerances increase iteration counts without affecting optimal values, indicating numerical stability of the decentralized scheme.

Overall, the framework exhibits economic sensitivity to uncertainty-budget calibration, while remaining robust and reproducible with respect to algorithmic parameters.

Table 6 evaluates scalability with respect to fleet size, scheduling horizon, and number of aggregators. Increasing fleet size from 2000 to 4000 and 6000 vehicles increases total solve time from 180 s to 355 s and 525 s, respectively, while ADMM iterations rise modestly from 130 to 134 and 138. This indicates that computational growth is primarily driven by expansion of local decision variables, whereas coordination complexity remains stable.

Extending the horizon from 24 h to 48 h and 72 h increases solve time to 365 s and 560 s, with iteration counts of 142 and 153. The increase is proportional to the number of time-indexed variables, yet convergence behavior remains stable. Introducing multiple aggregators increases coordination requirements. With two aggregators, iterations increase to 156 and solve time to 265 s. With three aggregators, iterations reach 171 and solve time 345 s. In the combined large-scale case (4000 vehicles, 48 h, two aggregators), iterations reach 188 and solve time 780s.

These results show near-linear growth in computational time with fleet size and horizon length, while iteration counts increase moderately with additional aggregators. The ADMM structure preserves convergence stability without centralized reformulation, supporting scalability to larger industrial–mobility systems.

REMARK 1

From a practical standpoint, the observed profit reduction for the aggregator and cost increase for the eco-industrial park under higher uncertainty budgets should be interpreted as risk management outcomes rather than structural disadvantages. In real-world electricity markets characterized by volatile wholesale prices, decision-makers rarely pursue purely profit-maximizing schedules without accounting for downside exposure. The results indicate that incorporating a bounded uncertainty budget enables both actors to internalize price risk in a controlled manner. For industrial operators and mobility service providers, this suggests that coordinated scheduling with embedded hedging mechanisms can support financially stable operation even when market conditions deteriorate. The framework therefore provides a structured decision-support tool for balancing expected returns against exposure to extreme price events.

REMARK 2

At the policy and market design level, the findings highlight the importance of preserving incentive compatibility in decentralized coordination schemes. Since both the aggregator and the eco-industrial park maintain positive economic outcomes across tested uncertainty levels, participation remains individually rational. This property is critical for real-world adoption, where entities operate under independent ownership and cannot be compelled to cooperate. The results suggest that regulators and market operators aiming to facilitate energy–mobility integration should prioritize mechanisms that allow bilateral contracting with embedded risk hedging, rather than imposing centralized optimization structures. Transparent risk allocation and voluntary participation are essential conditions for scalable deployment in competitive electricity markets.

6. CONCLUSION

This work addressed the coordination problem between a HDET aggregator and an EIP under simultaneous operational decentralization and electricity price uncertainty. The central challenge lay in enabling economically efficient interaction between independently owned entities while accounting for volatile locational marginal prices and stochastic fleet behavior, without violating privacy or scalability constraints. To resolve this, the study developed a decentralized coordination framework that integrates a hybrid distributionally robust and stochastic optimization structure with an ADMM-based solution mechanism, allowing each entity to optimize locally while remaining resilient to adverse market conditions.

The numerical results demonstrate that the proposed framework achieves consistent and economically meaningful outcomes across all examined scenarios. Under the hybrid DRO–SP formulation, coordinated scheduling successfully aligned charging, discharging, storage operation, and bilateral electricity exchange with wholesale price signals. Compared to deterministic pricing assumptions, robust price modeling induced conservative but stable decisions, shifting charging and storage actions toward periods with lower exposure to unfavorable price realizations. Sensitivity analysis revealed that expanding the electricity price uncertainty budget over the full daily horizon reduced the aggregator's net profit by approximately 41%, while increasing the EIP's operating cost by about 9%. These changes occurred smoothly, without feasibility loss, confirming that the optimization structure remains well-posed even under worst-case price deviations.

The results are fully consistent with the study's objectives of decentralized coordination, data privacy preservation, and robustness to market uncertainty. The ADMM-based scheme converged reliably, with residuals and economic indicators stabilizing after a finite number of iterations, confirming the feasibility of the distributed solution. The coupling between robust price signals and physical constraints, including fleet departure requirements and storage limits, produced realistic operating patterns across the electricity and gas subsystems. These outcomes are directly relevant to the operation of electrified freight facilities within industrial energy systems, where decision-making must remain resilient to adverse price conditions.

From a methodological standpoint, the study advances decentralized energy management by combining robust price modeling with stochastic fleet behavior, beyond conventional centralized or single-uncertainty formulations. The analysis is limited to a single-day horizon and fixed gas prices.

The present analysis is subject to several structural limitations. First, the scheduling horizon is restricted to a single day, which does not capture inter-day storage carryover effects or longer-term adaptive bidding behavior. Second, natural gas prices are assumed fixed, thereby excluding potential fuel price volatility and its interaction with electricity market dynamics. Third, the formulation abstracts from detailed transmission and distribution network constraints, including line congestion and voltage limitations, and instead focuses on energy balance and bilateral exchange at the interconnection point. As a result, spatial network impacts and congestion-induced price feedbacks are not represented. These modeling choices simplify tractability and highlight the coordination mechanism, yet they constrain the generalization of results to multi-period, fuel-volatile, and network-constrained environments.

Future work will extend the framework to multi-day scheduling, dynamic fuel price uncertainty, and coordination among multiple aggregators and interconnected industrial parks.

Declarations

Credit Author Statement

Peyman Zare: Conceptualization, Methodology, Software, Validation, Formal analysis, Investigation, Data Curation, Writing - Original Draft, Writing - Review & Editing, Visualization, Resources.

SeyedJalal SeyedShenava: Project Administration, Supervision, Formal analysis, Methodology, Writing - Review & Editing, Resources.

Hossein Shayeghi: Project Administration , Supervision, Formal analysis, Writing - Review & Editing. All authors have read and approved the paper.

Declaration of Competing Interest

The authors declare that they have no known competing financial interests or personal relationships that could have appeared to influence the work reported in this paper.

Conflict of Interest

The authors confirm that there is no conflict of interest associated with this publication.

Data Availability

The data that support the findings of this study are available from the corresponding author upon reasonable request.

Acknowledgement

This work is part of the current postgraduate research activities at the doctoral level and has been derived from the PhD thesis conducted by the first author, Peyman Zare, Ph.D. Candidate in Power Electrical Engineering, Department of Electrical Engineering, Faculty of Engineering, University of Mohaghegh Ardabili, Ardabil, Iran, under the supervision of Professor Seyed Jalal Seyed Shenava and the academic advisory of Full Professor Hossein Shayeghi.

Declaration of AI Assistance

The authors acknowledge that generative artificial intelligence tools (e.g., ChatGPT, Grammarly, and QuillBot) were used solely for language refinement, grammar correction, and stylistic improvement. No AI system contributed to the generation of research ideas, data analysis, results interpretation, or the scientific conclusions presented in this manuscript. The authors take full responsibility for the integrity, originality, and accuracy of the content.

Ethical Approval

This work did not involve any experiments with human participants or animals.

Funding

This work did not receive any specific grant from funding agencies in the public, commercial, or not-for-profit sectors.

Appendix A: Linear Reformulation of the Absolute-Value Term

The optimization problem associated with deviations in locational marginal prices exhibits nonlinearity due to the inclusion of an absolute-value term. To restore linear tractability without altering the underlying mathematical structure, this term is reformulated through an exact linear transformation. The approach relies on introducing auxiliary variables that split the deviation into its nonnegative components, together with a set of linear constraints that enforce equivalence with the original formulation. In this way, the nonlinear behavior is fully captured while preserving compatibility with linear and mixed-integer solvers. The reformulated relations governing the price deviation are summarized in Eqs. (A.1)-(A.5).

$$\pi_t^{\mathrm{worst},a} = \bar{\pi}_t^{\mathrm{exp},a} + \phi_t^{\pi-a} \tag{A.1}$$

$$\phi_t^{\pi-a} \leq \Delta_{\max^{AG}} \bar{\pi}_t^{\mathrm{exp},a} \tag{A.2}$$

$$\phi_t^{\pi-a} \geq -\Delta_{\max^{AG}} \bar{\pi}_t^{\mathrm{exp},a} \tag{A.3}$$

$$\phi_t^{\pi-a} - \phi_t^{+,\pi-a} + \phi_t^{-,\pi-a} = 0 \tag{A.4}$$

$$\sum_{t=1}^{T} \left(\phi_t^{+,\pi-a} + \phi_t^{-,\pi-a} \right) \leq \Gamma^p \tag{A.5}$$

Table B.1. Key technical and algorithmic settings of the case study.

Parameter Description	Assigned Value	Unit
HDET charging efficiency	0.92	–
HDET discharging efficiency	0.91	–
EIP storage charging efficiency	0.90	–
EIP storage discharging efficiency	0.89	–
Boiler thermal efficiency	0.86	–
CHP electrical efficiency	0.42	–
CHP thermal efficiency	0.47	–
Price uncertainty budget	12	–
ADMM convergence tolerance	0.001	–
Interconnection line capacity	55	MW
EIP storage maximum charging power	32	MWh
EIP storage maximum discharging power	32	MWh

APPENDIX B: INPUT PARAMETERS (TABLE B.1)

REFERENCES

[1] H. Shayeghi, P. Zare, I. F. Davoudkhani, and N. Bizon, “A comparative study of holistic expansion planning using osprey optimization algorithm for modern active electric distribution networks,” in *Proc. Int. Conf. Electron. Comput. Artif. Intell.*, pp. 1–7, 2024.

[2] A. Karam and J. Rich, “Planning the transition to electric trucks: An optimization framework for line-haul logistics,” *Res. Transp. Bus. Manag.*, vol. 61, p. 101413, 2025.

[3] A. Alonso-Villar, B. Davíðsdóttir, H. Stefánsson, E. I. Ásgeirsson, and R. Kristjánsson, “Optimising fast-charging infrastructure for long-haul electric trucks in remote regions under adverse climate conditions,” *ETransportation*, vol. 24, p. 100414, 2025.

[4] D. Speth, P. Plötz, and M. Wietschel, “An optimal capacity-constrained fast charging network for battery electric trucks in Germany,” *Transp. Res. Part A Policy Pract.*, vol. 193, p. 104383, 2025.

[5] T. Dimatulac, H. Maoh, and R. Carriveau, “Electricity demand assessment and charging infrastructure planning for long-haul electric vehicle operations in Ontario, Canada,” *Transp. Policy*, vol. 178, p. 103970, 2026.

[6] S. Johansson, D. Jung, and C. Sundström, “Cost-effective routing of a single heavy-duty battery electric truck,” *IFAC-PapersOnLine*, vol. 59, pp. 31–36, 2025.

[7] E. Mahyari and N. Freeman, “Electric vehicle fleet charging management: An approximate dynamic programming policy,” *Eur. J. Oper. Res.*, vol. 327, pp. 263–279, 2025.

[8] O. Anderson, N. Yu, W. Hong, and B. Wang, “Impact of flexible and bidirectional charging in medium- and heavy-duty trucks on California’s decarbonization pathway,” *Appl. Energy*, vol. 377, p. 124450, 2025.

[9] A. Golab, C. Loschan, S. Zwickl-Bernhard, and H. Auer, “The value of flexibility of commercial electric vehicle fleets in the redispatch of congested transmission grids,” *Energy*, vol. 316, p. 134385, 2025.

[10] A. Syla, D. Parra, and M. K. Patel, “Assessing flexibility from electric vehicles using an open-source energy system model: Trade-offs between smart charging, vehicle-to-grid and an extensive charging infrastructure,” *Energy*, vol. 326, p. 136236, 2025.

[11] Q. Wang, C. Huang, C. Wang, K. Li, and M. Shafie-khah, “Risk-averse frequency regulation strategy of electric vehicle aggregator considering multiple uncertainties,” *Appl. Energy*, vol. 382, p. 125259, 2025.

[12] A. Pradana, M. M. Haque, and M. Nadarajah, “A comprehensive framework for harnessing energy arbitrage benefits through an electric vehicle aggregator,” *J. Energy Storage*, vol. 139, p. 118617, 2025.

[13] T. Robbiano, M. Fresia, M. Caliano, and S. Bracco, “Optimal energy management strategies for aggregators in renewable energy communities,” *Int. J. Electr. Power Energy Syst.*, vol. 172, p. 111085, 2025.

[14] X. Audet, K. Qako, and A. Lesage-Landry, “A distributionally robust optimization strategy for virtual bidding in two-settlement electricity markets,” *Sustain. Energy Grids Netw.*, vol. 43, p. 101904, 2025.

[15] Z. Siqin, R. Diao, and M. Zhao, “Two-stage distributionally robust bidding strategies for multi-energy virtual power plants in energy, reserve and carbon markets,” *Energy*, vol. 334, p. 137455, 2025.

[16] W. Li, F. Dong, Z. Ji, and P. Wang, “Internal and external coordinated distributionally robust bidding strategy of virtual power plant operator participating in day-ahead electricity spot and peaking ancillary services markets,” *Appl. Energy*, vol. 386, p. 125514, 2025.

[17] W. Shen, H. Ding, M. Zeng, and X. Zhang, “Optimal bidding strategy for integrated energy system participating in spot power market: A wasserstein metric based DRO method,” *Energy*, vol. 327, p. 136402, 2025.

[18] X. Lei, H. Yu, J. Zhong, Z. Shao, and L. Jian, “A data-driven robust optimal day-ahead bidding strategy considering V2G operation for distribution-system-side virtual power plant,” *Energy*, vol. 338, p. 138795, 2025.

[19] S. Fatemi, A. Ketabi, and S. A. Mansouri, “A Bi-level distributed optimization framework to unlock flexibility in grid-connected energy storage systems and electric vehicle fleets,” *J. Energy Storage*, vol. 140, p. 119107, 2025.

[20] W. N. Tayari, Y. Merrad, S. B. Elghali, and M. Benbouzid, “Privacy-preserving ADMM-Based multi-agent energy sharing framework between communities using ring signature multi-party computation,” *Energy Rep.*, vol. 14, pp. 3783–3794, 2025.

[21] A. Quteishat, M. A. Younis, S. R. Seyednouri, and A. Safari, “Privacy-preserving and stochastic energy management of multi-microgrid systems with bidirectional electric vehicle integration,” *Renew. Energy Focus*, vol. 56, p. 100784, 2026.

[22] C. Wang, X. Li, R. I. Usmonovich, A. K. Rakhimovich, and X. Li, “Emission-aware energy management for smart buildings and energy hubs: A pathway to climate-neutral cities,” *Sustain. Cities Soc.*, vol. 136, p. 107059, 2026.

[23] Y. Wang, Z. Fan, Y. Z. Alharthi, S. Huang, and S. A. Mansouri, “Towards carbon-neutral energy systems: A two-layer robust model for day-ahead scheduling of emission-aware microgrids,” *Sustain. Cities Soc.*, vol. 131, p. 106764, 2025.

[24] S. S. Fazlhashemi, M. E. Khodayar, M. Sedighizadeh, and M. Khodayar, “Risk-averse operation of microgrids in distribution systems with price-responsive demands,” *Int. J. Electr. Power Energy Syst.*, vol. 168, p. 110581, 2025.

[25] J. Zhang, Z. Liang, L. Guan, W. Lu, C. Jiang, and X. Zeng, “Distributed multiple time scales energy management strategy for microgrid cluster with electric vehicles participation,” *Electr. Power Syst. Res.*, vol. 248, p. 111923, 2025.

[26] A. Kumar, A. Maulik, and K. A. Chinmaya, “A decentralized energy management scheme for a DC microgrid with correlated uncertainties and integrated demand response,” *Electr. Power Syst. Res.*, vol. 238, p. 111093, 2025.

[27] B. Ahmadi, A. Pappu, G. Hoogsteen, M. E. T. Gerards, and J. L. Hurink, “A novel user-centric decentralized multi-objective energy management system for energy communities,” *Sustain. Energy Grids Netw.*, vol. 44, p. 101936, 2025.

[28] S. S. Martín, F. García-Muñoz, F. Quezada, and S. Dávila, “User-centered decentralized P2P energy trading model for managing line congestion in energy communities,” *Sustain. Energy Grids Netw.*, vol. 44, p. 101931, 2025.

[29] A. Golshanfard, Y. Noorollahi, H. Hashemi-Dezaki, and H. Lund, “Mitigating emissions: Energy balancing in eco-industrial zones considering renewable energy and

electric vehicle uncertainties," *Renew. Energy Focus*, vol. 56, p. 100768, 2026.

[30] Y. Li, Z. Lu, X. Kong, Y. Cai, E. Du, and J. Zhang, "Robust planning of low-carbon energy transition in eco-power coupling system considering meteorological uncertainty," *Energy Convers. Manag.*, vol. 345, p. 120339, 2025.

[31] C. Fan, J. Wu, C. Zhang, Z. Zhu, J. Ma, and X. Zheng, "Coordinated optimization of logistics scheduling for electric logistics vehicles and energy management in integrated logistics parks with PV and ESS," *Energy*, vol. 341, p. 139296, 2025.

[32] P. Zare, H. Shayeghi, S. SeyedShenava, and B. Mohamadi, "Interactive scheduling for climate-neutral sustainable cities via carbon capture-enabled virtual energy communities considering digital-social welfare and joint certificate trading," *Sustain. Cities Soc.*, p. 107208, 2026.

[33] A. Mohammadian, A. Dejamkhooy, S. SeyedShenava, P. Zare, and B. Mohamadi, "Cross-sectoral synergy policy in climate-neutral sustainable cities with eco-friendly public transportation fleets and hydrogen-pivoted multi-energy transactions," *Energy*, p. 140296, 2026.

[34] H. Yang, P. You, and C. Shang, "Distributed planning of electricity and natural gas networks and energy hubs," *Appl. Energy*, vol. 282, p. 116090, 2021.

[35] J. Zhong, Y. Tan, Y. Li, Y. Cao, Y. Peng, Z. Zeng, Y. Nakanishi, and Y. Zhou, "Distributed operation for integrated electricity and heat system with hybrid stochastic/robust optimization," *Int. J. Electr. Power Energy Syst.*, vol. 128, p. 106680, 2021.

[36] P. Aliasghari, B. Mohammadi-Ivatloo, and M. Abapour, "Risk-based scheduling strategy for electric vehicle aggregator using hybrid stochastic/IGDT approach," *J. Clean. Prod.*, vol. 248, p. 119270, 2020.

[37] A. Najafi, A. Tavakoli, M. Pourakbari-Kasmaei, and M. Lehtonen, "A risk-based optimal self-scheduling of smart energy hub in the day-ahead and regulation markets," *J. Clean. Prod.*, vol. 279, p. 123631, 2021.

[38] P. Cai, C. Wen, B. Cao, and J. Qiao, "A wasserstein metric distributionally robust chance-constrained peer aggregation energy sharing mechanism for hydrogen-based microgrids considering low-carbon drivers," *Energy*, vol. 325, p. 136178, 2025.

[39] A. Najafi, H. Falaghi, J. Contreras, and M. Ramezani, "Medium-term energy hub management subject to electricity price and wind uncertainty," *Appl. Energy*, vol. 168, pp. 418–433, 2016.

[40] A. Mansour-Saatloo, M. Agabalaye-Rahvar, M. A. Mirzaei, B. Mohammadi-Ivatloo, M. Abapour, and K. Zare, "Robust scheduling of hydrogen based smart micro energy hub with integrated demand response," *J. Clean. Prod.*, vol. 267, p. 122041, 2020.